Vol 15 No 3, March 2006
1009-1963/2006/15(03)/0631-05

Chinese Physics

© 2006 Chin. Phys. Soc.
and IOP Publishing Ltd

Analytical analysis of surface potential for grooved-gate MOSFET*

Zhang Xiao-Ju(张晓菊)†, Gong Xin(龚 欣),
Wang Jun-Ping(王俊平), and Hao Yue(郝 跃)

Key Laboratory of Ministry of Education for Wide Band-Gap Semiconductor Materials and Devices, Microelectronics Institute, Xidian University, Xi'an 710071, China

(Received 26 July 2005; revised manuscript received 28 December 2005)

The improvement of the characteristics of grooved-gate MOSFETs compared to the planar devices is attributed to the corner effect of the surface potential along the channel. In this paper we propose an analytical model of the surface potential distribution based on the solution of two-dimensional Poisson equation in cylindrical coordinates utilizing the cylinder approximation and the structure parameters such as the concave corner θ_0. The relationship between the minimum surface potential and the structure parameters is theoretically analysed. Results confirm that the bigger the concave corner, the more obvious the corner effect. The corner effect increases the threshold voltage of the grooved-gate MOSFETs, so the better is the short channel effect (SCE) immunity.

Keywords: surface potential, corner effect, grooved-gate MOSFET
PACC: 7280C, 7340R, 7360J

1. Introduction

As the miniaturization of MOSFETs proceeds, the size of semiconductor devices goes into the deep-sub-micron regime. However, it is also found that short channel effect (SCE), drain induced barrier lowering (DIBL) and time dependent dielectric breakdown (TDDB) could not be sufficiently suppressed at 0.1μm gate-length.

In order to improve device reliability, the source/drain junction depths, gate dielectric and channel doping should be adjusted according to the empirical scaling rule. Consequently, such device parameters will approach physical and technological limits that are determined by the tunnel leakage current through the gate oxide, the increasing junction resistance, and the difficulty in reducing the ion-implantation energy.

Grooved-gate MOSFET is regarded as a promising structure to overcome the effects mentioned above. Several studies[1−5] have reported that the decrease of surface potential at the channel corner, which is called the corner effect, can improve the characteristics of the grooved-gate devices obviously, especially the reduction of short channel effect. Some results based on the simulation have already qualitatively analysed the corner effect.

The present paper proposes an analytical model for the surface potential, its minimum value and respective position based on the solution of 2D Poisson equation in cylindrical coordinates. The analysis takes into account the structure parameters (θ_0, $L_{\rm p}$), the doping concentration of the substrate and the gate and drain bias. The influence of the corner effect on the device characteristics is explained.

2. Model

Grooved-gate MOSFET, in which the gate electrode is placed on a groove separating the source and drain regions, is shown in Fig.1.

*Project supported by the National Natural Science Foundation of China (Grant No 603776024).
†E-mail: zh_xiaoju@sohu.com

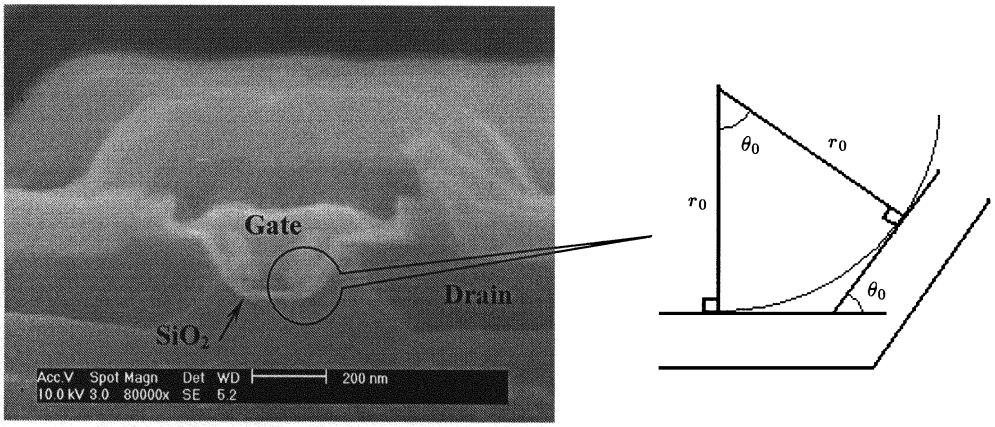


Fig.1. SEM image of the cross section of grooved-gated MOSFET and the concave corner with cylindrical approximation.

We assume that the concave corner is a part of a cylinder (Fig.1), where the corner radius of the convex groove is $r_0 = \dfrac{L_{\rm P}}{2\left(1+\tan\theta_0/2\right)}$.[6] The Poisson equation[7] for the potential in cylindrical coordinates is given by

$$\frac{\partial^2\varphi\left(r,\theta\right)}{\partial r^2}+\frac{1}{r}\frac{\partial\varphi\left(r,\theta\right)}{\partial r}+\frac{1}{r^2}\frac{\partial^2\varphi\left(r,\theta\right)}{\partial\theta^2}=\frac{qN_{\rm A}}{\varepsilon_{\rm Si}}, \quad (1)$$

where $\varphi\left(r,\theta\right)$ is the potential distribution, $N_{\rm A}$ is the doping concentration of the bulk silicon (assumed to be uniform), $L_{\rm P}$ is the length of the planar part of the channel and the other symbols are taken from those widely used in the literature.

The potential distribution in the depletion layer is assumed to be a parabolic profile[8] in the radial direction and is given by

$$\varphi\left(r,\theta\right)=C_0\left(\theta\right)+C_1\left(\theta\right)r+C_2\left(\theta\right)r^2, \quad (2)$$

where the coefficients $C_i\,(i=0,1,2)$ are functions of θ only. The three boundary conditions required for the solution are listed below.

(1) The potential at the edge of the depletion layer is the substrate bias,

$$\varphi\left(r=r_0+t_{\rm ox}+x_{\rm d}\right)=V_{\rm BS}. \quad (3a)$$

(2) The electric field at the edge of the depletion layer is zero,

$$\left.\frac{\partial\varphi}{\partial r}\right|_{r=r_0+t_{\rm ox}+x_{\rm d}}=0. \quad (3b)$$

(3) The electric field at the silicon/oxide interface can be derived from the gate potential ($V_{\rm g}$), the surface potential ($\varphi_{\rm s}\left(\theta\right)$), and gate oxide thickness.

$$\left.\frac{\partial\varphi}{\partial r}\right|_{r=r_0+t_{\rm ox}}=\frac{\varepsilon_{\rm ox}}{\varepsilon_{\rm Si}}\left(\frac{V_G-V_{\rm FB}-\varphi_{\rm s}\left(\theta\right)}{r_0\ln\left(1+t_{\rm ox}/r_0\right)}\right)$$
$$=M\left(V_{\rm g}-\varphi_{\rm s}\left(\theta\right)\right), \quad (3c)$$

where $x_{\rm d}$ is the depletion layer thickness for weak inversion which is approximately equal to $x_{\rm d}=\sqrt{\dfrac{2\varepsilon_{\rm Si}}{qN_{\rm A}}1.5V_{\rm B}}$, and $V_{\rm B}$ is the Fermi potential. The gate oxide capacitance per unit area[6] of the pie-shaped region in the corner is given as $C_{\rm oxc}=\dfrac{\varepsilon_0\varepsilon_{\rm ox}}{r_0\ln\left(1+t_{\rm ox}/r_0\right)}$, $M=\dfrac{\varepsilon_{\rm ox}}{\varepsilon_{\rm Si}}\left(\dfrac{1}{r_0\ln\left(1+t_{\rm ox}/r_0\right)}\right)$, $V_{\rm g}=V_{\rm G}-V_{\rm FB}$, $V_{\rm FB}$ being the flatband voltage.

Substituting Eq.(3) with these values into Eq.(2), $C_i\,(i=0,1,2)$ are obtained as

$$C_0=V_{\rm BS}-M\frac{\left(r_0+t_{\rm ox}+x_{\rm d}\right)^2}{2x_{\rm d}}\left(V_{\rm g}-\varphi_{\rm s}\left(\theta\right)\right),$$
$$C_1\left(\theta\right)=M\frac{r_0+t_{\rm ox}+x_{\rm d}}{x_{\rm d}}\left(V_{\rm g}-\varphi_{\rm s}\left(\theta\right)\right),$$
$$C_2\left(\theta\right)=-\frac{1}{2x_{\rm d}}M\left(V_{\rm g}-\varphi_{\rm s}\left(\theta\right)\right),$$

and the potential can be obtained

$$\varphi\left(r,\theta\right)=V_{\rm BS}+M\left(V_{\rm g}-\varphi_{\rm s}\left(\theta\right)\right)\left[-\frac{\left(r_0+t_{\rm ox}+x_{\rm d}\right)^2}{2x_{\rm d}}+\frac{r_0+t_{\rm ox}+x_{\rm d}}{x_{\rm d}}r-\frac{1}{2x_{\rm d}}r^2\right]. \quad (4)$$

Using this potential, Poisson equation can be solved at the surface of the channel, $r = r_0 + t_{ox}$, $\varphi(r = r_0 + t_{ox}, \theta) = \varphi_s(\theta)$,

$$\frac{\partial^2 \varphi_s}{\partial \theta^2} + \frac{1}{\lambda^2}\left(V_g - \varphi_s(\theta) - \frac{1}{M}\frac{(r_0 + t_{ox})\, x_d}{(x_d - r_0 - t_{ox})}\frac{qN_A}{\varepsilon_{Si}}\right) = 0, \tag{5}$$

where $\frac{1}{\lambda^2} = \frac{2(r_0 + t_{ox})(x_d - r_0 - t_{ox})}{x_d^2}$.

Simplifying Eq.(5), we have

$$\frac{d^2 \Phi(\theta)}{d\theta^2} - \frac{\Phi(\theta)}{\lambda^2} = 0, \tag{6}$$

where

$$\Phi(\theta) = \varphi_s(\theta) - V_g + \frac{1}{M}\frac{(r_0 + t_{ox})\, x_d}{(x_d - r_0 - t_{ox})}\frac{qN_A}{\varepsilon_{Si}}. \tag{7}$$

Some researchers[9] have verified that the potential barrier adjacent to the source is not affected by the drain potential. So the minimum value of the surface potential should appear near the source, and we must deal with Eq.(6) near the source region. It is reasonable to assume that on passing the source corner, the surface potential increases by $V_D/2$. The boundary conditions required for solving Eq.(6) are

$$\Phi(0) = V_{bi} - V_g + \frac{1}{M}\frac{(r_0 + t_{ox})\, x_d}{(x_d - r_0 - t_{ox})}\frac{qN_A}{\varepsilon_{Si}} = \Phi_s,$$

$$\Phi(\theta_0) = \left(V_{bi} + \frac{V_D}{2}\right) - V_g + \frac{1}{M}\frac{(r_0 + t_{ox})\, x_d}{(x_d - r_0 - t_{ox})}\frac{qN_A}{\varepsilon_{Si}} = \Phi_s + \frac{V_D}{2}.$$

On solving Eq.(7) using the above boundary conditions, we obtain

$$\Phi(\theta) = \frac{1}{\sinh\left(\frac{\theta_0}{\lambda}\right)}\left[\left(\Phi_s + \frac{V_D}{2}\right)\sinh\left(\frac{\theta}{\lambda}\right) + \Phi_s \sinh\left(\frac{\theta_0 - \theta}{\lambda}\right)\right]; \tag{8}$$

the surface potential

$$\varphi_s(\theta) = V_g - \frac{1}{M}\frac{(r_0 + t_{ox})\, x_d}{(x_d - r_0 - t_{ox})}\frac{qN_A}{\varepsilon_{Si}} + \frac{1}{\sinh\left(\frac{\theta_0}{\lambda}\right)}\left[\left(\Phi_s + \frac{V_D}{2}\right)\sinh\left(\frac{\theta}{\lambda}\right) + \Phi_s \sinh\left(\frac{\theta_0 - \theta}{\lambda}\right)\right]. \tag{9}$$

We have derived the minimum surface potential $\varphi_{s\,min}$ under the condition $d\varphi_s/d\theta|_{\theta=\theta_m} = 0$, where θ_m is given by

$$\theta_m = \frac{\lambda}{2}\ln\left(\frac{\Phi_s\left(e^{\frac{\theta_0}{\lambda}} - 1\right) - \frac{V_D}{2}}{\Phi_s\left(1 - e^{-\frac{\theta_0}{\lambda}}\right) + \frac{V_D}{2}}\right), \tag{10}$$

and the potential at θ_m becomes

$$\varphi_{s\,min} = V_g - \frac{qN_A}{\varepsilon_{ox}} r_0 \ln\left(1 + \frac{t_{ox}}{r_0}\right)\frac{(r_0 + t_{ox})x_d}{(x_d - r_0 - t_{ox})} + \frac{1}{\sinh\frac{\theta_0}{\lambda}}\sqrt{\left(\Phi_s\left(e^{\frac{\theta_0}{\lambda}} - 1\right) - \frac{V_D}{2}\right)\left(\Phi_s\left(1 - e^{-\frac{\theta_0}{\lambda}}\right) + \frac{V_D}{2}\right)}. \tag{11}$$

From Eq.(8), it can be seen that λ describes the potential distribution in the depletion layer, which in turn depends on the device geometry and boundary conditions. To operate the device as in the long channel regime, i.e., to avoid the short channel effect, the minimum channel potential should be as small as possible. This minimum channel potential can be decreased by increasing the substrate doping concentration or by reducing λ. The definition of λ implies that the bigger the corner angle θ_0, the smaller the radius r_0 and the smaller the λ, which is called the corner effect of the grooved-gate devices.

3. Results and discussion

We assumed a doping concentration of 10^{20}cm^{-3} for the source and drain (N_D), $N_A = 10^{16}\text{cm}^{-3}$, V_G=0.7V, V_D=0.05V and $L_P = 0.1\mu$m, then V_{bi} = 0.93V, V_{FB}=0.3V.

Figure 2 shows the relationship between the grooved corner and the radius for the grooved-gate MOSFETs. The results clearly indicate that a smaller value of concave corner gives a lower r_0 value and thus

good device characteristics.

The surface potential distributions along the channel of the source corner are given in Fig.3 for θ_0=15°, 30°, 45°, 60°, 75°, 90°. It is clear that the surface potential decreases obviously for a relatively bigger corner angle. Because of the degradation of the surface potential, higher gate voltage is necessary to ensure that the channel is open. So the threshold voltage of the grooved-gate MOSFETs is higher than the planar devices of which the threshold voltage decreases with the decrease of the channel length, which makes the devices operate as in the long channel regime and shows a good resistance to short channel effect. This result is in good agreement with the simulated results and experimental data.[4,10] Because of the corner effect, the potential barrier for electron flow from source to drain will increase, and then the potential barrier which is effective in suppressing the short channel effect degrades the drain current characteristics as compared with the planar devices.[10]

The corner effect of grooved-gate devices can be explained as follows: The smaller the radius of the corner, the more dispersive the electric field lines according to the theory of electric field. Because the radius of the planar part of the channel can be regarded as infinite, the electric field at the corner is very small, and the collapses of the surface potential form the barriers.

Figure 3 also shows that no minimum potential point appears in the distribution line when the corner is smaller than a critical angle. This indicates that when the corner angle is too small, no potential barrier exists and the characteristics of the grooved-gate devices are analogous to that of the planar ones. When it is bigger than the critical angle, the corner effect will be observed.

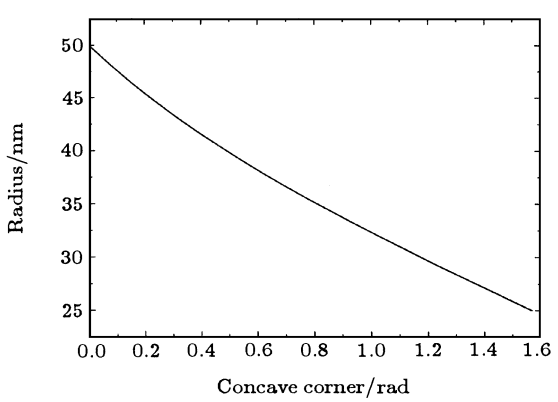


Fig.2. Relationship between the grooved corner and the radius.

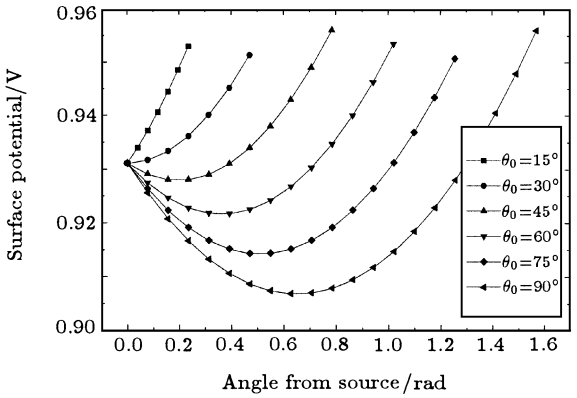


Fig.3. Surface potential distribution for different corner values.

Results concerning the potential barrier height ($\varphi_{s\,min}$) and its respective position (θ_m) in the channel region as a functions of the corner angle are plotted in Fig.4. The minimum potential data and the position are determined from Eqs.(10) and (11). From Fig.4 it can be noted that the minimum surface potential decreases with the increase of the corner angle. It can be explained analogously as the above: the bigger the corner angle, the smaller the radius and the more heavily the surface potential collapses, giving rise to the increase of the threshold voltage and the reduction of the short channel effect. It also can be observed that θ_m, at which the minimum potential occurs, increases with increasing corner angle; and the minimum potential seems to appear at almost the same position, i.e. the corner of the channel (Fig.1).

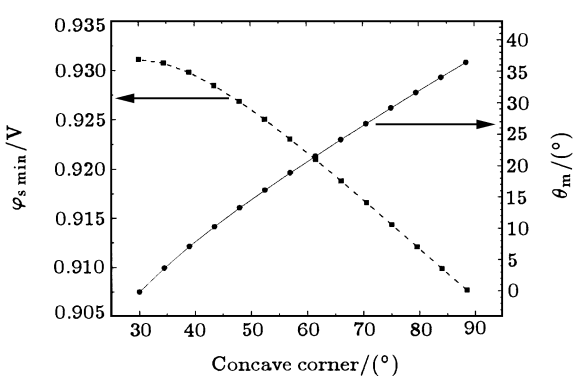


Fig.4. Formation of potential barrier height (minimum surface potential) and their respective position as a function of groove corner.

4. Conclusion

An analytical model has been derived for the minimum surface potential for grooved-gate MOSFETs.

The relationship between groove corner and surface potential showed that it is possible to construct a lower value of surface potential by increasing the corner angle, thus increasing the threshold voltage and reducing the short channel effect.

References

[1] Tanaka J, Toyabe T, Ihara S, Kimura S, Noda H and Itoh K 1993 *IEEE Electron Devices Letters* **14** 396

[2] Ren H X and Hao Y 2001 *Chin. Phys.* **10** 189

[3] Ren H X, Hao Y and Xu D G 2000 *Acta Phys. Sin.* **49** 1241 (in Chinese)

[4] Ren H X and Hao Y 2000 *Acta Phys. Sin.* **49** 1683 (in Chinese)

[5] Tong J N, Zou X C and Shen X B 2004 *Acta Phys. Sin.* **53** 2905 (in Chinese)

[6] Zhang X J, Ren H X, Feng Q and Hao Y 2004 *Chin. J. Semiconductors* **25** 441 (in Chinese)

[7] Kranti A, Haldar S and Gupta R S 2000 *Asia-Pacific Microwave Conference* (Sydney) p880

[8] Kranti A, Haldar S and Gupta R S 2001 *Microelectronics Engineering* **56** 241

[9] Goodwin S H and Plummer J D 1984 *IEEE Trans. Electron Devices* **ED-31** 861

[10] Zhang X J, Ma X H, Ren H X, Hao Y and Sun B G 2005 *Chin. J. Semiconductors* **26** 197 (in Chinese)